Journal of Alloys and Compounds 488 (2009) 223–226

Contents lists available at ScienceDirect

Journal of Alloys and Compounds

journal homepage: www.elsevier.com/locate/jallcom

Non-equilibrium alloy formation in the Ag–Zr system by ion beam mixing

Y.Y. Cui, T.L. Wang, K.P. Tai, B.X. Liu*

Advanced Materials Laboratory, Department of Materials Science and Engineering, Tsinghua University, Beijing 100084, China

ARTICLE INFO

Article history:
Received 2 July 2009
Received in revised form 28 July 2009
Accepted 28 July 2009
Available online 25 August 2009

Keywords:
Ag–Zr alloy
Ion beam mixing
Metastable crystalline phase
Amorphous phase

ABSTRACT

Based on Miedema's model, a Gibbs free energy diagram was first constructed for the Ag–Zr system and showed that the free energy of the Ag–Zr multilayered films could be higher than that of the corresponding supersaturated solid solutions and amorphous phase. Ion beam mixing with $Ag_{90}Zr_{10}$, $Ag_{48}Zr_{52}$ and $Ag_{12}Zr_{88}$ multilayered films was then conducted by 200 keV xenon ions. It was found that an fcc supersaturated solid solution, a mixture of fcc and hcp metastable crystalline structures and an hcp supersaturated solid solution were formed and that amorphous phases were also observed to coexist with the metastable crystalline structures. The experimental observations concerning the non-equilibrium alloy formation matched well with the calculated Gibbs free energy diagram.

1. Introduction

During the past decades, some non-equilibrium materials processing techniques, such as mechanical alloying, ion beam mixing, vapor deposition, pulse laser deposition, vapor quenching and high-pressure alloying have been developed and proved to be very effective in producing non-equilibrium alloys [1–5]. Moreover, many alloys obtained from these processes have shown unique properties in a number of respects and have become potential for practical applications [6–10]. In particular, ion beam mixing (IBM) of multilayered films has been well recognized as a powerful means for producing non-equilibrium materials in the binary metal systems [7,8,11,12]. There are three essential features involved in the IBM scheme. Firstly, the individual layer thicknesses of the metal–metal multilayered films could be designed to be a couple of nanometers, so that the interfacial free energy of the initial multilayered films could be elevated to a highly energetic state, surpassing that of a specific non-equilibrium alloy of interest. Secondly, ion irradiation could be conducted to trigger the interfacial mixing at low temperatures. Thirdly, the irradiation dose could be finely varied by adjusting the ion current density, thus enabling one to trace the detailed process in the non-equilibrium alloy formation. Till now, some 100 binary metal systems have been studied and a great number of non-equilibrium alloys have been obtained by IBM [11–14]. Meanwhile, in recent years, theoretical studies have also been performed to establish relevant model for explaining the formation of the non-equilibrium alloys. A number of excellent research works have been published in the literature. For instance, Miedema's model and Alonso's method have been proposed as a thermodynamic approach to explain or predict the formation of the non-equilibrium alloys. Concerning the alloy phase formation and transformation, a Gibbs free energy diagram of a system calculated based on Miedema's model and Alonso's method could give a relevant criterion of the relative stabilities of the possible alloy phases in the system under consideration [11,15,16].

In the present study, we focused on the Ag–Zr system characterized by a negative heat of formation $\Delta H_f = -31$ kJ/mol [15], since the Ag-based alloys are widely used in industry as electrical contact materials, welding materials, catalyzed materials, antibacterial and medical materials, etc. [17–20], while the addition of Zr and some other elements has been proved to be an effective measure for further improving the performance of Ag-based alloys [21]. Up to now, the Ag–Zr system has been studied by some researchers [22–26] and the Ag–Zr equilibrium phase diagram [27] has well been constructed, which helps the design of alloy composition. However, only a few experimental investigations directly show the interaction between Ag and Zr under non-equilibrium conditions and the detail of non-equilibrium alloy formation is still an open issue. It is therefore of interest to study the non-equilibrium alloy formation in Ag–Zr system by IBM, which is far-from-equilibrium. In the present study, thermodynamic calculation was first conducted based on the Miedema's model and Alonso's method and IBM experiment was then conducted to study the formation of possible non-equilibrium alloys in the Ag–Zr system.

* Corresponding author. Tel.: +86 10 6277 2557; fax: +86 10 6277 1160.
E-mail address: dmslbx@tsinghua.edu.cn (B.X. Liu).

0925-8388/$ – see front matter © 2009 Elsevier B.V. All rights reserved.
doi:10.1016/j.jallcom.2009.07.188

2. Thermodynamic calculation and experimental procedures

2.1. Thermodynamic calculation

Generally, the Gibbs free energy of an alloy phase can be calculated by:

$$\Delta G = \Delta H - T \cdot \Delta S \quad (1)$$

where ΔH and ΔS are the enthalpy and entropy terms, respectively. As a first approximation, the entropy term for a concentrated solid solution (CSS) or an amorphous phase is simply taken as that of an ideal solution, i.e.:

$$\Delta S = -R[c_A \ln c_A + c_B \ln c_B] \quad (2)$$

where R is the gas constant and c_A and c_B are the atomic concentrations of metals A and B, respectively.

According to Miedema's model and Alonso's method [15,16], the enthalpy change ΔH is the sum of three terms:

$$\Delta H = \Delta H^c + \Delta H^e + \Delta H^s \quad (3)$$

where ΔH^c, ΔH^e and ΔH^s corresponding to the chemical, elastic, and structural contributions, respectively. The chemical term ΔH^c is closely related to the electron redistribution generated at the boundary for the Wigner–Seitz unit cell when alloying, and can be calculated by:

$$\Delta H^c = c_A c_B [c_B \Delta \bar{H}^{inter}_{A\,in\,B} + c_A \Delta \bar{H}^{inter}_{B\,in\,A}] \quad (4)$$

where $\Delta \bar{H}^{inter}_{A\,in\,B}$ and $\Delta \bar{H}^{inter}_{B\,in\,A}$ are the solution enthalpies of A solved in B and that of B solved in A, respectively. The elastic term ΔH^e for a CSS is caused by the atomic size mismatch of the two constituent metals and can be expressed by taking the weighted average of the mismatch energies:

$$\Delta H^e = c_A c_B [c_B \Delta \bar{H}^{elastic}_{A\,in\,B} + c_A \Delta \bar{H}^{elastic}_{B\,in\,A}] \quad (5)$$

where $\Delta \bar{H}^{elastic}_{A\,in\,B}$ and $\Delta \bar{H}^{inter}_{B\,in\,A}$ are the partial elastic mismatch energies for A solved in B and B solved in A, respectively. The structure term ΔH^s is deduced from the lattice stability $E(Z)$ of the bcc, fcc, and hcp structures as a function of the number of valence electrons Z of the metal:

$$\Delta H^s = E(Z) - [c_A E(Z_B) + c_B E(Z_A)] \quad (6)$$

where $E(Z)$, $E(Z_A)$, and $E(Z_B)$ are the lattice stability of the CSS and pure metals A and B, and Z, Z_A, and Z_B are the mean numbers of valence electrons of the CSS and the numbers of valence electrons of pure metals A and B, respectively.

For an amorphous phase, both elastic and structural terms are absent in the enthalpy of formation. According to Miedema's model [15], the enthalpy of the amorphous phase is therefore given by:

$$\Delta H^{amorphous} = \Delta H^c + \alpha \cdot (c_A T_{m,A} + c_B T_{m,B}) \quad (7)$$

Here α is an empirical constant, being 3.5 J/(mol K). $T_{m,i}$ is the melting point of the component.

For an A–B multilayered film, the Gibbs free energy of the initial state should be calculated by adding the interfacial free energy to the ground state (i.e., the zero line) representing a mechanical mixture of A and B in the bulk form [28]. The excess interfacial free energy of the multilayered film can be calculated by:

$$\Delta G_{multi} = \alpha_A S_{fA} \gamma^{SS}_{BA} + \alpha_B S_{fB} \gamma^{SS}_{AB} \quad (8)$$

where S_{fA} and S_{fB} are the surface areas occupied by one mole of atoms A and B, respectively. α_A and α_B are the fraction of the interfacial atoms A and B versus the total number of atoms in the A–B multilayered film. γ^{SS}_{AB} (or γ^{SS}_{BA}) is the interfacial free energy of one mole of atoms A (or B) solved in B (or A). These terms can easily be calculated following the well-documented literature [15,16,28].

By comparing the Gibbs free energy of multilayered film with those possible forming phases, such as solid solutions, amorphous phase, a reasonable explanation can be given to the phase formation.

2.2. Experimental procedures of ion beam mixing

In the present study, 200 keV xenon ions were used as irradiating ions in the IBM. According to the TRIM program [29], the total thickness of the Ag–Zr multilayered films was designed to be 40 nm to match the range of the irradiating ions. Three sets of Ag–Zr multilayered films with overall compositions of $Ag_{90}Zr_{10}$, $Ag_{50}Zr_{50}$ and $Ag_{10}Zr_{90}$ were designed and the Ag–Zr multilayered films consisted of totally 6, 11 and 5 layers, respectively. The desired overall compositions of the samples were obtained by adjusting the relative thicknesses of the individual Ag and Zr layers and the individual layer thicknesses of both Ag and Zr were accordingly calculated. The Ag–Zr multilayered films were prepared by alternatively depositing pure Ag (99.99%) and Zr (99.99%) onto newly cleaved NaCl single crystals as substrates in an ultra-high vacuum electron-beam evaporation system, and the background vacuum level was better than 10^{-6} Pa. An in situ quartz oscillator was employed to monitor the thickness of the metal layers and the deposition rate was controlled to be about 0.5 Å/s.

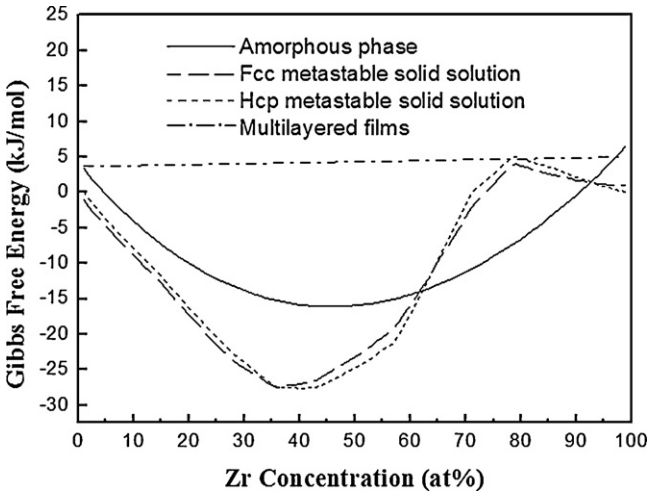

Fig. 1. Calculated Gibbs free energy diagram of the Ag–Zr system.

The as-deposited Ag–Zr multilayered films were then irradiated in an implanter by 200 keV xenon ions with a vacuum level better than 5×10^{-4} Pa and the irradiation dose was in a range from 6×10^{14} Xe^+/cm^2 to 5×10^{15} Xe^+/cm^2. During irradiation, the sample holder was always cooled by liquid nitrogen (77 K) and the ion current density was confined to be 0.5 μA/cm^2 to avoid an overheating effect. For structural characterization, all the Ag–Zr multilayered films were removed from the substrates by de-ionized water and put onto the Cu grids and then examined by room temperature transmission electron microscopy (TEM) to observe and identify the morphology and structural changes in the films. X-ray fluorescence examination was employed to determine the real compositions of the Ag–Zr multilayered films.

3. Results and discussion

We firstly present the results of the thermodynamic calculation. Based on Miedema's model and Alonso's method, a Gibbs free energy diagram of the Ag–Zr system was constructed, including the energy curves of the amorphous phase, fcc metastable solid solution and hcp metastable solid solution, respectively, and is shown in Fig. 1. One can see from Fig. 1, the free energy curve of the Ag–Zr multilayered films was higher than that of the corresponding metastable solid solutions and amorphous phase over the whole composition range, suggesting that supersaturated solid solutions or amorphous phase may appear under some appropriate non-equilibrium conditions.

We now present the results from IBM experiments. The real compositions of the Ag–Zr multilayered films were confirmed to be $Ag_{90}Zr_{10}$, $Ag_{48}Zr_{52}$ and $Ag_{12}Zr_{88}$, respectively. The results of non-equilibrium alloy formation in the Ag–Zr multilayered films subjected to irradiation to ion doses of 6×10^{14} Xe^+/cm^2, 1×10^{15} Xe^+/cm^2, 3×10^{15} Xe^+/cm^2 and 5×10^{15} Xe^+/cm^2, were listed in Table 1. The results showed that in general, metastable solid solution(s) were formed in the Ag–Zr multilayered films and amorphous phase was observed to coexist with the metastable crystalline phases.

Table 1
Structural phase transitions in the Ag–Zr multilayered samples upon 200 keV Xe ion beam mixing to various doses.

Dosage (Xe^+/cm^2)	$Ag_{90}Zr_{10}$	$Ag_{48}Zr_{52}$	$Ag_{12}Zr_{88}$
6×10^{14}	F	F+A	A+F
1×10^{15}	F	F+A	A+F
3×10^{15}	F	F+H	A+F+H
5×10^{15}	F	F+H	H

F: fcc metastable crystalline; H: hcp metastable crystalline; A: amorphous; +: indicates both phases are obtained.

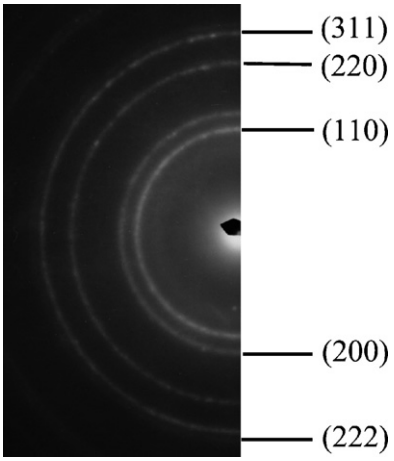

Fig. 2. The SAD patterns for the $Ag_{90}Zr_{10}$ multilayered film after an irradiation dose of 6×10^{14} Xe^+/cm^2.

For the $Ag_{90}Zr_{10}$ multilayered sample, Fig. 2 shows a selected area diffraction (SAD) pattern when the sample was irradiated to an ion dose of 6×10^{14} Xe^+/cm^2. One can see from Fig. 2 that an unique crystalline structure was obtained and it was indexed to be an fcc structure with a lattice parameter 4.10 Å, which is quite close to the lattice parameter of Ag (4.08 Å). Referring to the Ag–Zr equilibrium phase diagram [27], the solubility of Zr in Ag as well as the solubility of Ag in Zr is almost zero in the equilibrium state. The fcc crystalline structure obtained in the $Ag_{90}Zr_{10}$ sample should be an Ag-based supersaturated solid solution, meaning that a supersaturated solid solubility of Zr in Ag could at least be 10 at.%. Further increasing the irradiation dose, the SAD pattern of the $Ag_{90}Zr_{10}$ sample remained unchanged.

For the $Ag_{48}Zr_{52}$ sample, Fig. 3(a) and (b) shows the SAD patterns when the sample was irradiated to the ion doses of 6×10^{14} Xe^+/cm^2 and 3×10^{15} Xe^+/cm^2, respectively. One can see that one halo and some sharp diffraction rings coexisted in the pattern in Fig. 3(a), indicating an incomplete amorphous phase was formed in the sample. The diffraction rings were indexed to be an fcc crystalline structure, with a lattice parameter $a = 4.09$ Å. When the

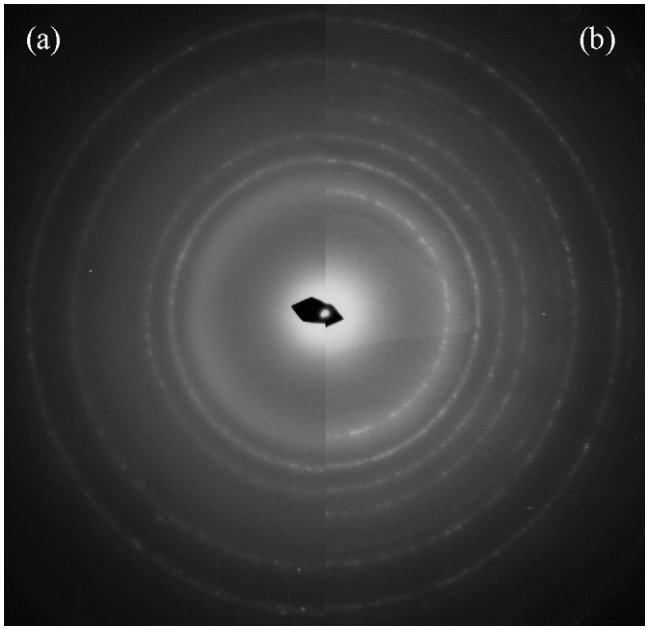

Fig. 3. The SAD patterns for $Ag_{48}Zr_{52}$ multilayered films after irradiation doses of (a) 1×10^{15} Xe^+/cm^2 and (b) 3×10^{15} Xe^+/cm^2.

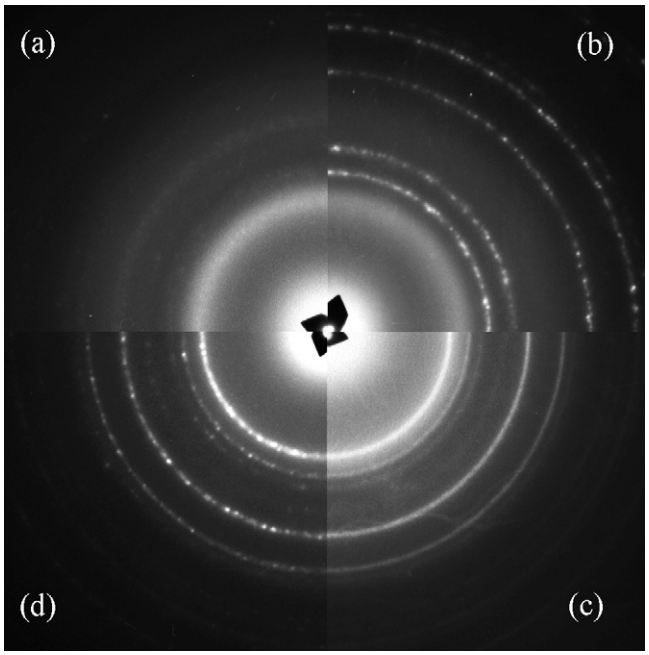

Fig. 4. The SAD patterns for $Ag_{12}Zr_{88}$ multilayered films after irradiation doses of (a) 6×10^{14} Xe^+/cm^2, (b) 1×10^{15} Xe^+/cm^2, (c) 3×10^{15} Xe^+/cm^2 and (d) 5×10^{15} Xe^+/cm^2.

irradiation dose was raised to 3×10^{15} Xe^+/cm^2, the diffraction rings of the fcc structure retained, while the halo disappeared and another set of diffraction rings emerged, as shown in Fig. 3(b). The newly emerged diffraction rings were indexed to be an hcp crystalline structure, with lattice constants of $a = 3.20$ Å and $c = 5.12$ Å. The coexistence of the fcc and hcp metastable crystalline structure remained unchanged in the $Ag_{48}Zr_{52}$ sample up to an irradiation dose of 5×10^{15} Xe^+/cm^2.

For the $Ag_{12}Zr_{88}$ sample, Fig. 4(a)–(d) shows the SAD patterns when the sample was irradiated to ion doses of 6×10^{14} Xe^+/cm^2, 1×10^{15} Xe^+/cm^2, 3×10^{15} Xe^+/cm^2 and 5×10^{15} Xe^+/cm^2, respectively. In Fig. 4(a), a large diffused halo together with one very weak diffraction ring were displayed, indicating a dominant amorphous phase and a trace of crystalline structure were obtained in the $Ag_{12}Zr_{88}$ sample irradiated at a dose of 6×10^{14} Xe^+/cm^2. Increasing the irradiation does to 1×10^{15} Xe^+/cm^2, the intensity of the diffused halo was decreased and a set of diffraction rings were clearly to be seen, as shown in Fig. 4(b). The diffraction rings were indexed to be from an fcc crystalline structure with a lattice parameter of 4.12 Å, suggesting a Ag-based metastable crystalline phase was formed. Further increasing the irradiation does to 3×10^{15} Xe^+/cm^2, another set of diffraction rings appeared while both the diffused halo and the fcc crystalline diffraction rings became weak, as evidenced by the SAD pattern shown in Fig. 4(c), implying that another crystalline structure began to form. Fig. 4(d) is the SAD pattern of the $Ag_{12}Zr_{88}$ sample when it was irradiated at a dose of 5×10^{15} Xe^+/cm^2. It can clearly be seen from Fig. 4(d) that the fcc crystalline structure and the amorphous phase disappeared, leaving only the newly formed crystalline structure, which was identified to be an hcp Zr-based structural phase, with the lattice constants of $a = 3.20$ Å and $c = 5.11$ Å. Referring again to the Ag–Zr equilibrium phase diagram [27], the hcp crystalline structure obtained should be an hcp Zr-based supersaturated solid solution, meaning that a supersaturated solid solubility of Ag in Zr could at least be 12 at.%.

It is known that IBM of multilayered films is very effective in producing the non-equilibrium metallic alloys [7,8,11,12]. According to the atomic collision theory [30], the IBM process can generally be divided into two steps, i.e., the first step of atomic collision cas-

cade triggered by impinging ions and followed by a second step of relaxation. In the first step, as the energy of the irradiating Xe^+ was 200 keV, while the binding energy of the solids was 5–10 eV, which was several magnitudes of order smaller than that of the irradiating ions, consequently, a sequence of ballistic collision was triggered in the Ag–Zr multilayered films. The atomic collision cascade was responsible for the inter-mixing of Ag and Zr by inducing the interfacial diffusion of Ag atoms into its partner Zr lattices and vise versa, resulting in a highly energetic Ag–Zr mixture. In the second step of relaxation, the highly energetic Ag–Zr mixture should relax towards equilibrium. According to the atomic collision theory, the relaxation period was extremely short, approximately 10^{-10} to 10^{-9} s [11,30], only very minor atomic rearrangement could take place. Consequently, either simple structured crystalline phase, such as fcc, bcc and hcp, could be grown or the disordered structure preferred to preserve, thus forming an amorphous phase. For the relaxation step, the equilibrium thermodynamics came into play to govern the direction of relaxation as well as to indicate what kind of possible states for the atomic mixture to reside in. Accordingly, in the IBM experiments, fcc supersaturated solid solution, a mixture of fcc and hcp metastable crystalline structures and hcp supersaturated solid solution were observed in three sets of Ag–Zr multilayered films, whereas amorphous phase was observed to coexist with some metastable crystalline structures under some irradiation conditions. The experimental observations concerning the non-equilibrium alloy formation in the Ag–Zr system matched well with the calculated Gibbs free energy diagram shown in Fig. 1.

4. Conclusions

For the Ag–Zr system characterized by a negative heat of formation $\Delta H_f = -31$ kJ/mol, thermodynamic calculation suggested that the free energy of the Ag–Zr multilayered films could be higher than that of the corresponding supersaturated solid solutions and amorphous phase. Ion beam mixing experiments showed that Ag-based fcc supersaturated solid solution and Zr-based hcp supersaturated solid solution could both be obtained with supersaturated solid solubilities to be 10–12 at.%, which was significantly greater than almost zero observed in the Ag–Zr equilibrium phase diagram. Interestingly, amorphous phase was also observed to coexist with some metastable crystalline structures.

Acknowledgements

The authors are grateful to the financial support from the National Natural Science Foundation of China (50531040 and 50871058), The Ministry of Science and Technology of China (2006CB605201), and the Administration of Tsinghua University.

References

[1] C.C. Koch, O.B. Cavin, C.G. McKamey, J.O. Scarbrough, Appl. Phys. Lett. 43 (1983) 1017.
[2] B.X. Liu, W.L. Johnson, M.A. Nicolet, S.S. Lau, Appl. Phys. Lett. 42 (1983) 45.
[3] K. Sumiyama, Y. Yoshitake, Y. Nakamura, Acta Mater. 33 (1985) 1785.
[4] H.U. Krebs, Int. J. Non-Equilibr. Process. (UK) 10 (1997) 3.
[5] N. Dubrovinskaia, L. Dubrovinsky, I. Kantor, W.A. Crichton, V. Dmitriev, V. Prakapenka, G. Shen, L. Vitos, R. Ahuja, B. Johansson, I.A. Abrikosov, Phys. Rev. Lett. 95 (2005) 245502.
[6] D. Bonyuet, G. Gonzalez, J. Ochoa, F. Gonzalez-Jimenez, L. D'Onofrio, J. Alloys Compd. 434 (2007) 442.
[7] R. De Bastiani, A.M. Piro, M.G. Grimaldi, E. Rimini, G.A. Baratta, G. Strazzulla, Appl. Phys. Lett. 92 (2008) 241925.
[8] G.A. Muller, E. Carpene, R. Gupta, P. Schaaf, K. Zhang, K.P. Lieb, Eur. Phys. J. B 48 (2005) 449.
[9] E. Nunes, E.C. Passamani, C. Larica, J.C.C. Freitas, A.Y. Takeuchi, E. Baggio-Saitovitch, A.C. Doriguetto, A.A.R. Fernandes, Mater. Sci. Eng. A 390 (2005) 13–18.
[10] M. Pisarek, M. Janik-Czachor, A. Gebert, A. Molnar, P. Kedzierzawski, B. Rac, Appl. Catal. A 267 (2004) 1.
[11] B.X. Liu, W.S. Lai, Q. Zhang, Mater. Sci. Eng. R 29 (2000) 1.
[12] T.L. Wang, J.H. Li, K.P. Tai, B.X. Liu, Scripta Mater. 57 (2007) 157.
[13] I.L. Graff, S.R. Teixeira, L. Amaral, M.C.M. Alves, W.H. Flores, J. Appl. Phys. 96 (2004) 1469.
[14] N. Ding, T.L. Wang, K.P. Tai, J.H. Li, X. He, Y. Dai, B.X. Liu, J. Alloys Compd. 476 (2009) 253.
[15] F.R. de Boer, R. Boom, W.C.M. Mattens, A.R. Miedema, A.K. Niessen, Cohesion in Metals: Transition Metal Alloys, North Holland, Amsterdam, 1988.
[16] J.A. Alonso, L.J. Gallego, J.A. Somoza, Nuovo Cimento 12 (1990) 587.
[17] A. Inoue, M. Kai, S. Hoshi, T. Izumi, Y. Shiohara, K. Murata, M. Otsuka, Physica C 412 (2004) 1060.
[18] J.-W. Yoon, S.-B. Jung, J. Alloys Compd. 458 (2008) 200.
[19] O. Akhavan, M. Abdolahad, R. Asadi, J. Phys. D: Appl. Phys. 42 (2009) 135416.
[20] D. Lee, R.E. Cohen, M.F. Rubner, Langmuir 21 (2005) 9651.
[21] X.C. He, Y.M. Wang, H.S. Liu, Z.P. Jin, J. Alloys Compd. 417 (2006) L1.
[22] K.G. Zhang, H.Z. Zhao, Y.H. Zhou, J. Less Common Met. 138 (1988) 173.
[23] R.V. Patil, J. Nucl. Mater. 187 (1992) 197.
[24] O. Taguchi, Y. Iijima, Mater. Trans. JIM 35 (1994) 673.
[25] H. Okamoto, J. Phase Equilibr. 18 (1997) 312.
[26] A. Kulińska, B. Wodniecka, P. Wodniecki, J. Alloys Compd. 426 (2006) 76.
[27] T.B. Massalski, H. Okamoto, P.R. Subramanian, L. Kacprzak, Binary Alloy Phase Diagrams, second ed., ASM International, Ohio, 1990.
[28] Z.J. Zhang, O. Jin, B.X. Liu, Phys. Rev. B 51 (1995) 8076.
[29] J.F. Ziegler, J.P. Biersack, U. Littmark, The Stopping and Range of Ions in Solids, Pergamon Press, New York, 1992.
[30] M.W. Thompson, Defects and Radiation Damage in Metals, Cambridge Press, Cambridge, 1969.